

## 8A.5 Verification of Supercell Cold Pools in High-Resolution WRF Simulations using StickNet In Situ Data

Anthony E. Reinhart<sup>1\*</sup>, Christopher C. Weiss<sup>1</sup>, and David C. Dowell<sup>2</sup>

<sup>1</sup>Department of Geosciences,  
Atmospheric Science Group, Texas Tech University  
Lubbock, Texas

<sup>2</sup>National Center for Atmospheric Research (NCAR)  
Boulder, Colorado

### 1. INTRODUCTION

Numerical weather prediction (NWP) simulations of deep convection have traditionally overestimated the magnitude of the resulting cold pool (Gilmore and Wicker 1998; Dawson et al. 2010; James and Markowski 2010). While the bias can be related to many physical parameterizations, the microphysical parameterizations are suspected to cause the largest proportion of the bias. The biases present have been suggested to be dependent upon the mesoscale environment, in particular the relative humidity above cloud base (Gilmore and Wicker 1998; James and Markowski 2010).

Radar data have been assimilated fairly regularly into NWP models for storm scale dynamics (e.g., Dowell and Bluestein 1997; Dowell et al. 2004; Dowell and Wicker 2009; Tanamachi et al. 2009; Dawson et al. 2010). These data have a high temporal and spatial resolution that are a valuable asset in simulating storm scale features. Frequently, Doppler velocity and reflectivity are assimilated by means of an ensemble Kalman filter (EnKF). The EnKF provides a way to ingest the radar data into the model by modifying the pressure and temperature fields (Dowell and Wicker 2009).

During VORTEX2, high spatial and temporal resolution observations of supercell thunderstorm thermodynamics were gathered. Two example cases (11 June 2009 and 18 May 2010) were chosen from the data set. The two events have similar environmental profiles and are compared in this study.

This study will address the supercell cold pool bias using the Weather Research and Forecasting (WRF) model and EnKF data assimilation technique. StickNets, rapidly deployable in situ

instruments capable of measuring thermodynamic and kinematic data at high frequencies, will be used to verify the numerically simulated cold pool (Schroeder and Weiss 2008; Weiss and Schroeder 2008). Twenty-four StickNets were operational during the VORTEX2 field campaign.

### 2. Cases Considered

#### a. 11 June 2009

On 11 June 2009 VORTEX2 intercepted two supercells east of Pueblo, CO near La Junta, CO. The supercells initiated off of preexisting boundaries to the west several hours before intercept. The two supercells passed within 50 km of the Pueblo WSR-88D (KPUX). VORTEX2 sampled the supercells from approximately 2355 UTC through 0245 UTC. StickNets were deployed between 0111 UTC and 0241 UTC. The supercell updrafts passed through the StickNet array at 0132 UTC.

Mobile soundings launched from the NCAR MGAUS teams showed an environment favorable for supercells (Fig. 1). The environment has a moderate dry layer above the cloud base level between 700 hPa and 650 hPa. The drier air above cloud base leads to stronger entrainment the formation of strong evaporatively driven downdrafts, which can lead to stronger cold pools (Gilmore and Wicker 1998). However, it has been found that when using ice microphysics the low relative humidity above the cloud base cause lower evaporational rates, which results in weaker cold pools (James and Markowski 2010).

#### b. 18 May 2010

On 18 May 2010 VORTEX2 teams intercepted a long-lived and cyclic supercell as it propagated through northern Texas between 2230 UTC and 0130 UTC. StickNets were deployed between 2222 UTC and 2302 UTC with the supercell updraft crossing the array near 2330 UTC.

---

\* Corresponding author address: Anthony E. Reinhart, Texas Tech University, Atmospheric Science Group, Department of Geosciences, Lubbock, TX 79409; anthony.reinhart@ttu.edu

StickNets captured thermodynamic and kinematic state variables over the width of the storm. This coverage featured 1.5 km spacing, except a 6 km gap where StickNets could not be deployed in the city of Dumas.

Mobile soundings launched from the inflow environment show a sounding with a dry layer above the cloud base between 750 hPa and 600 hPa (Fig. 2). This structure is similar to the sounding from 11 June 2009.

### 3. METHODOLOGY

Real data simulations were performed for the two events using the Advanced Research Weather Research and Forecasting model (WRF) (Skamarock et al. 2005). The Data Assimilation Research Testbed (DART) was used to assimilate WSR-88D radar data into the numerical simulation (Anderson et al. 2009). Initial conditions were taken from the North American Mesoscale model (NAM). A total of 16 members were used in this study.

Simulations have a horizontal grid point resolution of 3 km. The horizontal domain size is approximately 200 km x 150 km, centered on La Junta, CO for 11 June 2009, and Dumas, TX for 18 May 2010. 55 vertical levels were used starting near the surface and stretching to 10.0 hPa.

Physics used in the model include the Noah land surface model, YSU planetary boundary layer scheme, RRTM radiation scheme with Dudhia shortwave parameterization and two different microphysical parameterizations, the single moment Purdue Lin scheme (Lin et al. 1983) and the newly implemented Milbrandt and Yau two moment scheme (Milbrandt and Yau 2005, 2006a, 2006b). The Lin scheme is a six hydrometeor class scheme, including water vapor, cloud water, ice, snow, hail/graupel, and rain. The Milbrandt and Yau scheme is a two moment scheme solving for number concentration and mixing ratio. Seven classes of hydrometeors are included in this scheme, including those mentioned in the Lin scheme plus graupel.

Objective analysis was performed on the WSR-88D data before being assimilated into DART. A 3 km Cartesian grid with the same dimensions of the model domain was used. The radar data were treated as point observations, and the points retained their altitudes as the analysis interpolated them onto the grid. Radar data that were below 0 dBZ were then increased to 0 dBZ.

A single pass Cressman scheme was used on the data to yield the final objectively analyzed data field (Fig. 3).

The WSR-88D data were assimilated into the model every 2 min during the entire integration period of the two events. The radar data were perturbed with an additive noise scheme (Caya et al. 2005; Dowell and Wicker 2009), adding random noise to model field variables ( $u$ ,  $v$ , temperature, and dewpoint temperature) where reflectivity data were greater than 25 dBZ. Two radar fields were assimilated into the model: Clear-air reflectivity and Doppler velocity. Clear-air reflectivity is defined here as any area where the reflectivity is 0 dBZ. Clear-air reflectivity data were used to suppress spurious convection that occurs in the model.

To determine the bias of cold pools forecast by the numerical simulations, StickNet observations are used as truth. StickNets were deployed ahead of each target supercell with an average spacing of approximately 2 km, allowing for a high-resolution sampling of supercell thermodynamics.

StickNet observations of the event are manipulated in two ways. First, a 12-second time average is passed over the data. A time-to-space conversion over ten minutes is performed and then the converted observations are objectively analyzed. The objective analysis performed on the StickNet data is a Barnes single pass method (Trapp and Doswell 2000). The resulting StickNet data are then be used to verify the numerical simulations (Fig. 4).

Verification of the strength of the supercell cold pool is accomplished in two manners. The supercell is divided into sections (forward flank and rear flank) and air mass average deficits are calculated and compared to the StickNet data. Also, maximum deficits within the aforementioned simulations will be compared to the StickNet maximum deficits. The sub storm verification will provide insight into the structure of errors within supercell cold pools that can only now be resolved due to the wide spatial coverage and fine spacing of the StickNets.

In this study four numerical simulations were performed (two for each case) to assess the biases in cold pools produced by the two microphysical parameterizations and to develop a framework for further statistical verification of supercell cold pools in a sub storm manner.

## 4. MODEL RESULTS

### *a. 11 June 2009*

Simulations of the 11 June 2009 La Junta Colorado storm began at 2100 UTC and ended at 0300 UTC. The two moment microphysical parameterization has weaker reflectivity values (Fig. 5), which is due to a smaller concentration of rain occurring within the two moment microphysics scheme. Spatial errors with the single moment simulation are small ( $O(1\text{ km})$ ) while the two moment scheme yields a spatial error of about 20 km. Inflow soundings derived from the numerical simulations again closely match the observed inflow sounding (Fig. 6).

The simulated cold pool is 9 K (11 K) cooler than the simulated inflow environments for the double (single moment) schemes (Fig. 7). While the reflectivity of the two moment microphysical parameterization looks weaker the cold pool is fairly strong.

### *b. 18 May 2010*

The two simulations of the 18 May 2010 Dumas, Texas storm have a start time of 1800 UTC and integrate through 0300 UTC. The two moment Milbrandt and Yau scheme produces a weaker low level reflectivity product than the single moment Lin scheme (Fig. 8).

Model errors in the timing ( $\sim 15\text{ min}$ ) and position of the simulated storms are fairly small (less than 30 km). These errors are not degrading to the verification as the mode and storm evolution are similar to the observations. A model sounding taken from the inflow environment shows similar low level thermodynamic characteristics to the observed inflow sounding (Fig. 9), reinforcing the accuracy of the replicated mesoscale environment for both simulations.

The simulated cold pool is 10 K (12 K) cooler than the inflow environment (Fig. 10) for the two moment (single moment) microphysical scheme. This maximum deficit occurs within the forward flank of the supercell. The areal extent of the cold pool is much larger for the single moment case with a large portion of the forward flank at a 12 K deficit to the inflow (Fig. 10).

## 5. VERIFICATION

Verification of the simulated storms was undertaken when the storm achieved a similar maturity as the observed supercell sampled by StickNets. The assimilation of radar data and the use of ensembles ensure the simulation evolves closely to the observations and verification times are within a half-hour of the observed times. The forward flank is verified by comparing the one-minute averaged  $\theta_v$  derived from StickNet observations to  $\theta_v$  at the lowest model level within the forward flank. The rear flank verification is done in a similar manner. The base state is defined such that all deficits are taken from the inflow environment.

In general, the single moment parameterization generates a stronger cold pool than the two moment parameterization, and both are colder than the observations from the StickNet (Tables 1 and 2). The single moment parameterization produces a larger cold pool over a larger area than observed.

### *a. 11 June 2009*

The single moment simulation for 11 June 2009 has a cold pool maximum deficit of 11.43 K at a position within the forward flank but close to the mesocyclone. The average deficit within the forward flank is 7.73 K. The StickNet observations within the forward flank have an average deficit of 4.5 K. The rear flank deficit from the simulation is 6.15 K. Since, StickNet observations have a gap where the rear flank of the supercell propagated, verification of the simulation to the StickNet observations is not possible in this case.

The two moment parameterization produces a cold pool that has a maximum deficit of 8.3 K. The simulated average deficit of the forward flank is 6.19 K, which is closer to the observations than the single moment deficits. The rear-flank average deficit is 2.2 K, which is much warmer than the single moment deficit.

### *b. 18 May 2010*

For the Dumas, TX simulation with the single moment parameterization, the strongest part of the cold pool was located within the forward flank and had a  $\theta_v$  deficit of 11.45 K. At a similar time, and likewise located within the forward flank, StickNet observations recorded a deficit of 6.0 K. The

forward flank-average  $\theta_v$  deficit of the simulated supercell is 6.6 K. Average StickNet observations in the forward flank are 4 K below the observed inflow  $\theta_v$ . The rear flank portion of the simulated supercell has an average deficit of 4.1 K, while StickNet rear-flank observations averaged 2.8 K cooler than the observed inflow environment.

The two moment microphysical simulation had a maximum cold pool deficit of 10.83 K located within the forward flank of the simulated supercell. The average deficit of the forward flank is 5.99 K with the strongest deficits towards the right side of the forward flank. The StickNet-average forward flank deficit for the verification time is 6.0 K. The two moment scheme clearly produces a more realistic cold pool. The rear flank air mass deficit is 2.27 K, which compared to the StickNet-sampled rear-flank air mass deficit, 2.2 K, shows again that the two moment scheme is accurate in this case.

## 6. CONCLUSIONS AND FUTURE WORK

Real data simulations were conducted using WRF with radar data assimilated into the model via DART. These simulations were performed to verify supercellular cold pools with high-resolution observations. Two cases from VORTEX2 were chosen because of the proximity of the event to a WSR-88D, suitable coverage of StickNet probes, and similar environmental soundings.

Numerical simulations thus far have a horizontal grid resolution of 3 km, which is still rather coarse. Simulations with a horizontal grid resolution of 1 km are planned. The higher resolution will allow for better scale since 1 km is necessary for directly resolving convective updrafts. The number of ensemble members will be increased to 50 to ensure a representative depiction of model uncertainty.

Even with the coarse resolution presented above, we can see a difference in thermodynamics between portions of the supercell. The forward flank is always colder than the rear flank. This difference is intuitive, but important to note. The strongest deficits remain close to the updraft in the single moment scheme, while they are more removed downshear from the updraft in the two moment scheme. These differences in placement and its implications on the modulation of buoyancy and vorticity will be studied further.

The verification technique developed and tested in this study will be used with the planned

high-resolution simulations. Other verification techniques will be used in conjunction to aid in determining the spatial errors and bias in the simulations.

## 7. ACKNOWLEDGEMENTS

The National Science Foundation (NSF) under grant AGS-0800542 funded this study. The authors are grateful for the assistance of Ryan Metzger, Bradley Charboneau, and Patrick Skinner provided when drafting and editing this document.

## 8. References

- Anderson, J., T. Hoar, K. Raeder, H. Liu, N. Collins, R. Torn, and A. Avellano, 2009: The Data Assimilation Research Testbed: A community facility. *Bull. of the Amer. Meteor. Soc.*, **90**, 1283-1296.
- Caya, A., J. Sun, and C. Snyder, 2005: A Comparison between the 4DVAR and the Ensemble Kalman Filter Techniques for Radar Data Assimilation. *Mon. Wea. Rev.*, **133**, 3081-3094.
- Dawson, D. T., M. Xue, J. A. Milbrandt, and M. K. Yau, 2010: Comparison of evaporation and cold pool development between single-moment and multimoment bulk microphysics schemes in idealized simulations of tornadic thunderstorms. *Mon. Wea. Rev.*, **138**, 1152-1171.
- Dowell, D. C., and H. B. Bluestein, 1997: The Arcadia, Oklahoma, storm of 17 May 1981: Analysis of a supercell during tornadogenesis. *Mon. Wea. Rev.*, **125**, 2562-2582.
- Dowell, D. C., and L. J. Wicker, 2009: Additive noise for storm-scale ensemble data assimilation. *J. Atmos. Oceanic Technol.*, **26**, 911-927.
- Dowell, D. C., F. Zhang, L. J. Wicker, C. Snyder, and N. A. Crook, 2004: Wind and temperature retrievals in the 17 May 1981 Arcadia, Oklahoma, supercell: Ensemble Kalman Filter Experiments. *Mon. Wea. Rev.*, **132**, 1982-2005.
- Gilmore, M. S., and L. J. Wicker, 1998: The influence of midtropospheric dryness on supercell morphology and evolution. *Mon. Wea. Rev.*, **126**, 943-958.
- James, R. P., and P. M. Markowski, 2010: A numerical investigation of the effects of

- dry air aloft on deep convection. *Mon. Wea. Rev.*, **138**, 140-161.
- Lin, Y.-L., R. D. Farley, and H. D. Orville, 1983: Bulk parameterization of the snow field in a cloud model. *J. Climate Appl. Meteor.*, **22**, 1065-1092.
- Milbrandt, J. A., and M. K. Yau, 2005: A multimoment bulk microphysics parameterization. part I: analysis of the role of the spectral shape parameter. *J. Atmo. Sci.*, **62**, 3051-3064.
- —, 2006a: A multimoment bulk microphysics parameterization. part III: control simulation of a hailstorm. *J. Atmo. Sci.*, **63**, 3114-3136.
- —, 2006b: A multimoment bulk microphysics parameterization. part IV: sensitivity experiments. *J. Atmo. Sci.*, **63**, 3137-3159.
- Schroeder, J. L., and C. C. Weiss, 2008: Integrating research and education through measurement and analysis. *Bull. Amer. Meteor. Soc.*, **89**, 793-798.
- Skamarock, W. C., J. B. Klemp, J. Dudhia, D. O. Gill, D. M. Barker, W. Wang, and J. G. Powers, 2005: A description of the Advanced Research WRF Version 2. *NCAR Technical Note*, 100.
- Tanamachi, R. L., D. C. Dowell, L. J. Wicker, H. B. Bluestein, S. J. Frasier, and K. Hardwick, 2009: Numerical simulations of a cyclic tornadic thunderstorm augmented by EnKF assimilation of mobile Doppler radar data. *Preprints, 34th Conference on Radar Meteorology*, Williamsburg, VA, Amer. Meteor. Soc.
- Trapp, R. J., and C. A. Doswell, 2000: Radar data objective analysis. *J. Atmos. Oceanic Technol.*, **17**, 105-120.
- Weiss, C. C., and J. L. Schroeder, 2008: The 2007 and 2008 MOBILE Experiment: Development and testing of the TTU StickNet platforms. *Preprints, 24th Conference on Severe Local Storms*, Savannah, GA, 5.1.

Table 1. 11 June 2009  $\theta_v$  Deficits

Deficits	Single Moment	Two Moment	StickNet Observations
Average Forward Flank	7.73 K	6.19 K	4.5 K
Average Rear Flank	6.15 K	2.2 K	n/a
Maximum	11.43 K	8.3 K	6.0 K

Table 2. 18 May 2010  $\theta_v$  Deficits

Deficits	Single Moment	Two Moment	StickNet Observations
Average Forward Flank	6.6 K	5.99 K	6.0 K
Average Rear Flank	4.1 K	2.27 K	2.2 K
Maximum	11.45 K	10.83 K	7.0 K

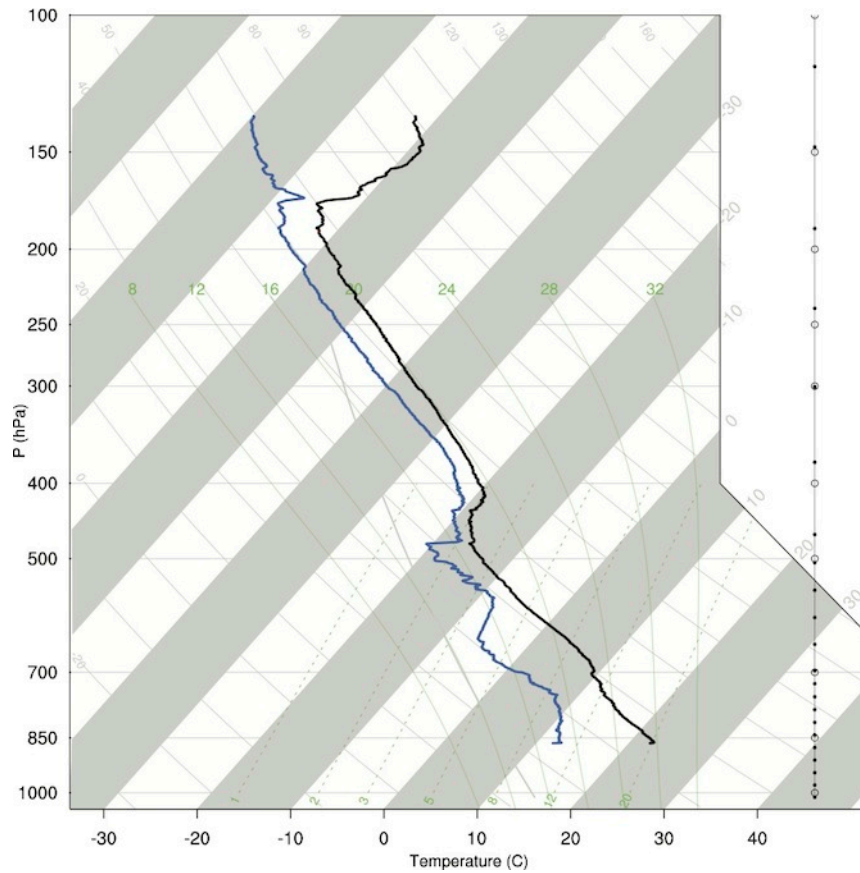


Fig. 1. Inflow sounding launched south of La Junta, CO at 0014 UTC.

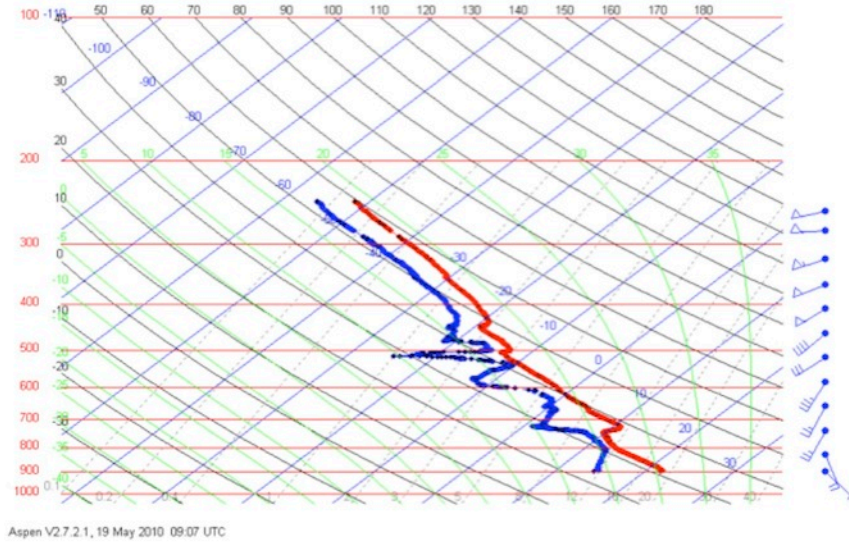


Fig. 2. Inflow sounding for 18 May 2010 launched at 2300 UTC near Stinnett, TX.

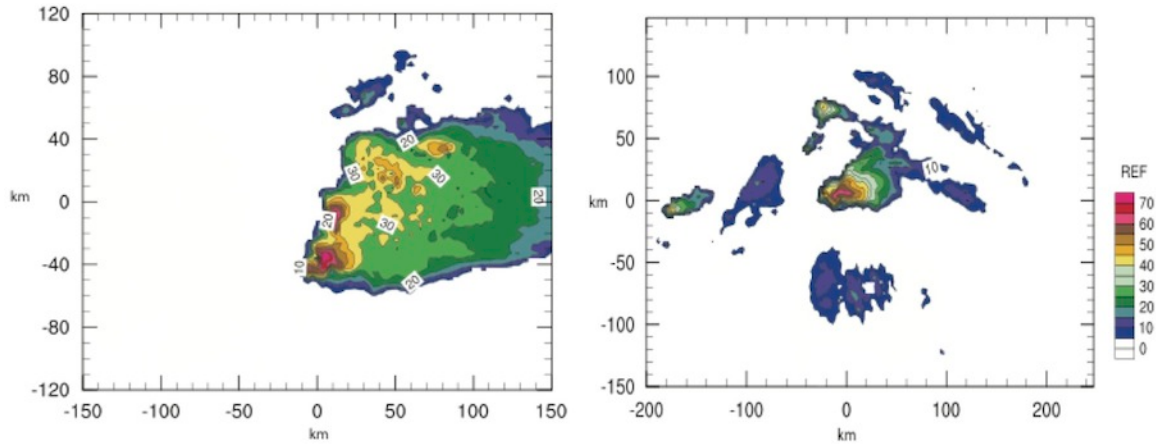


Fig. 3. Objectively analyzed WSR-88D data from 11 June 2010 (left) and 18 May 2010 (right).

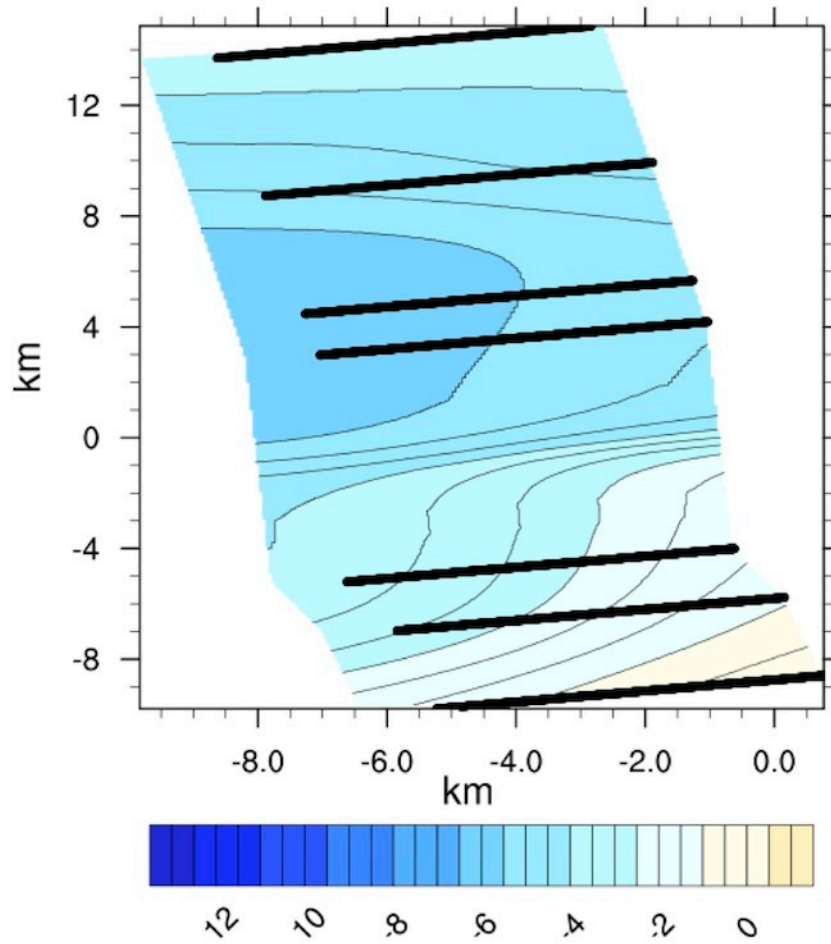


Fig. 4. An example of objectively analyzed StickNet data from 18 May 2010.  $\theta_v$  is contoured as a deficit to the inflow environment. The black lines indicate where StickNets observations (converted from time to space) are located.

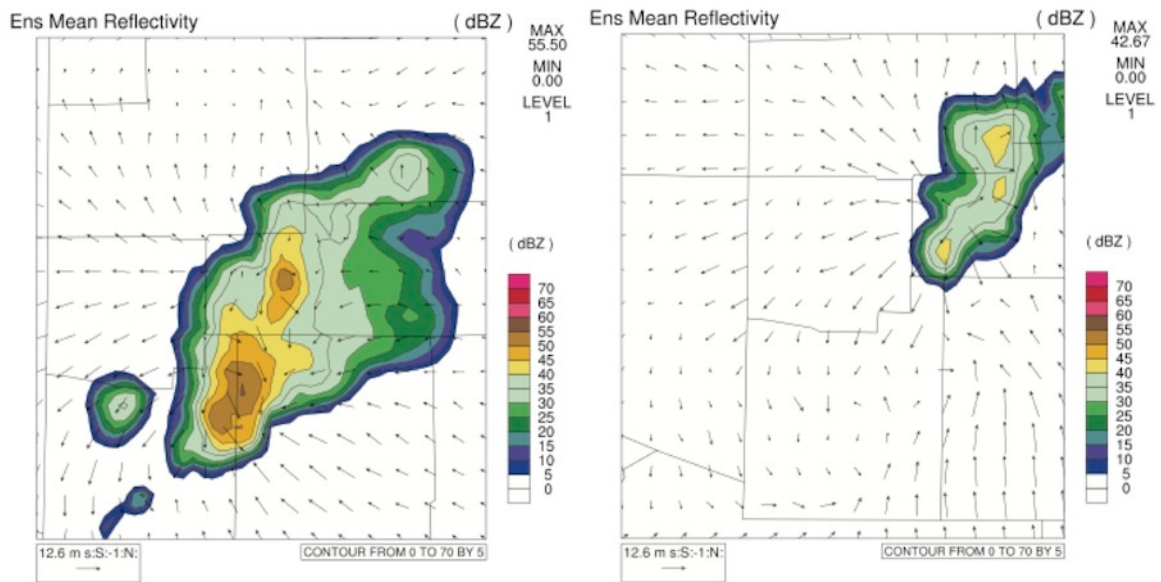


Fig. 5. 11 June 2009 simulated reflectivity (dBZ) of simulations utilizing the single moment (left) and the two moment (right) microphysical parameterizations at the verification time (0100 UTC).

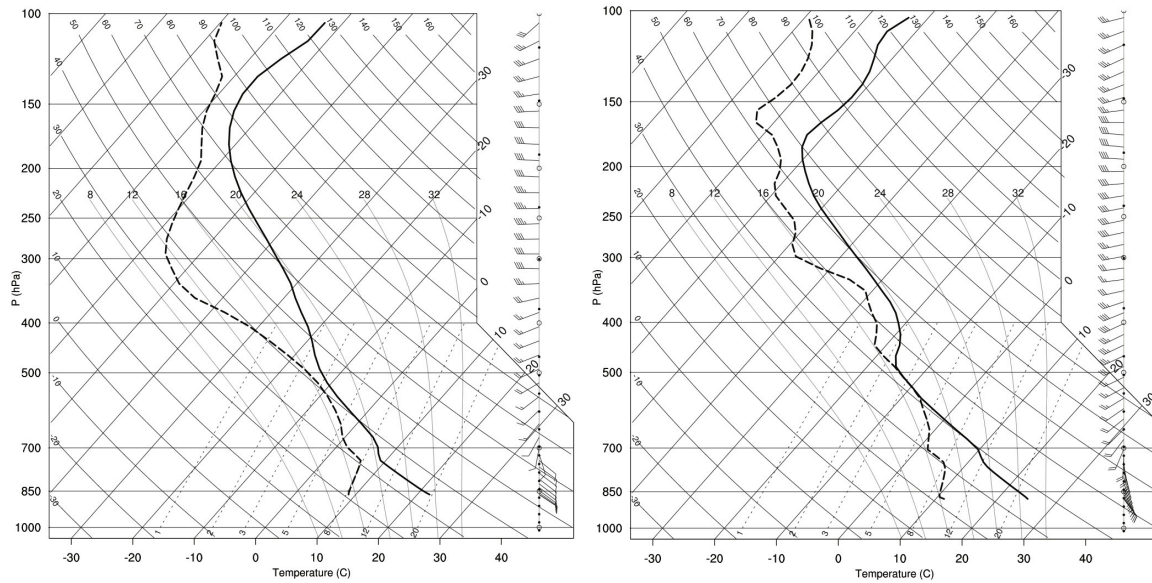


Fig. 6. Model derived soundings from 11 June 2009 of the inflow environment for simulations utilizing the single moment (left) and the two moment (right) microphysical parameterizations.

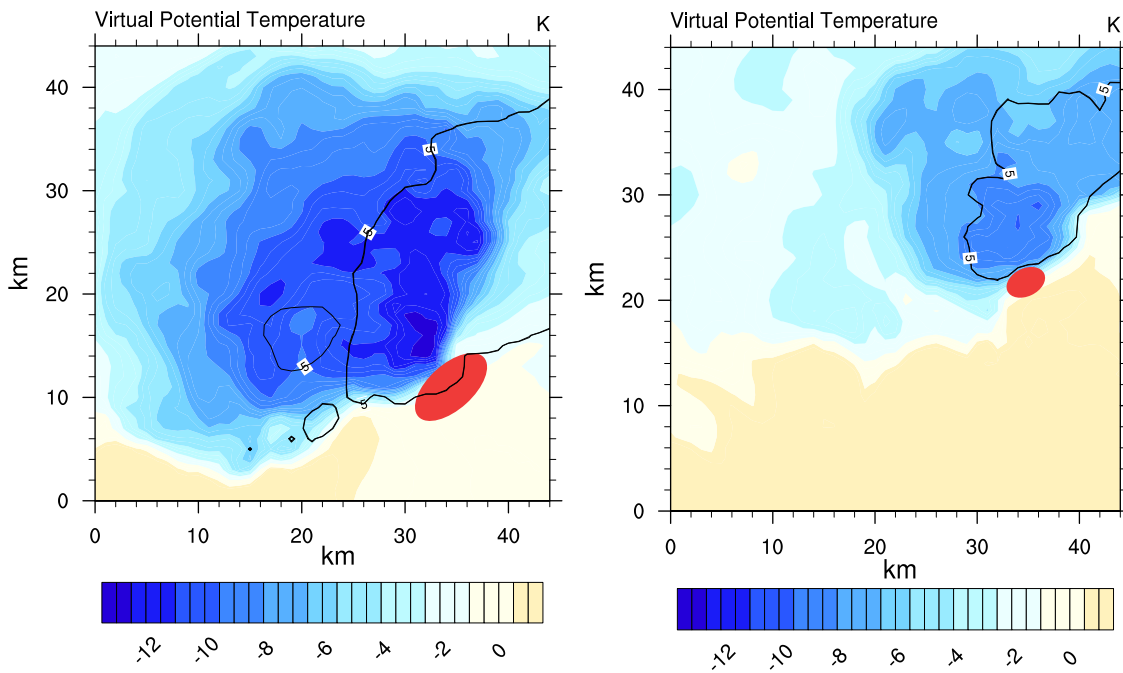


Fig. 7. Virtual potential temperature deficits (K) at the lowest model level for the 11 June 2009 simulations using the single moment (left) and the two moment (right) microphysical parameterizations. The verification time is 0100 UTC. The red oval indicates the location of the mesocyclone.

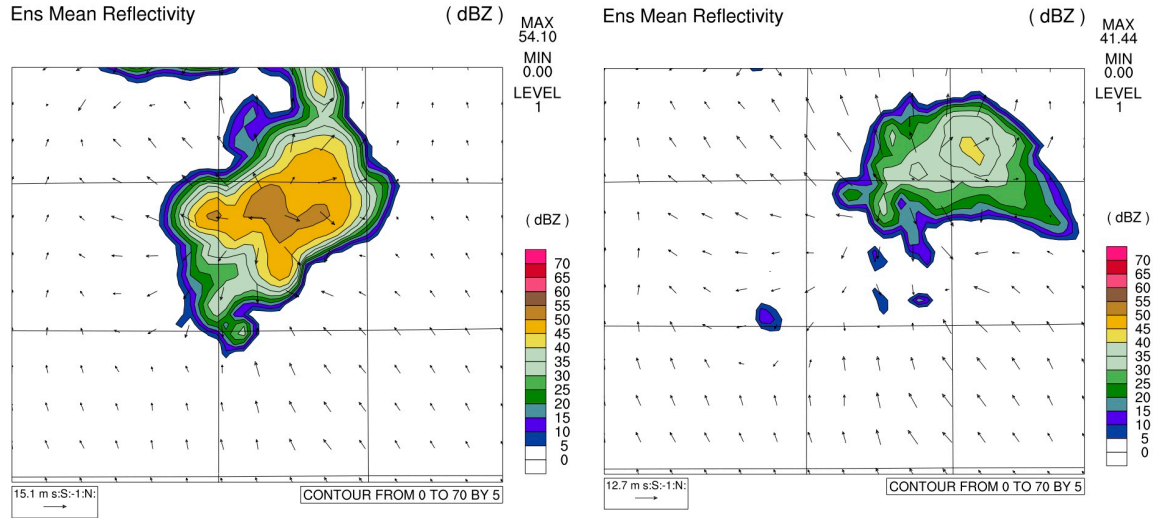


Fig. 8. Model simulated reflectivity (dBZ) of the 18 May 2010 supercell near Dumas, TX, using for the single moment (left) and two moment (right) microphysical parameterizations.

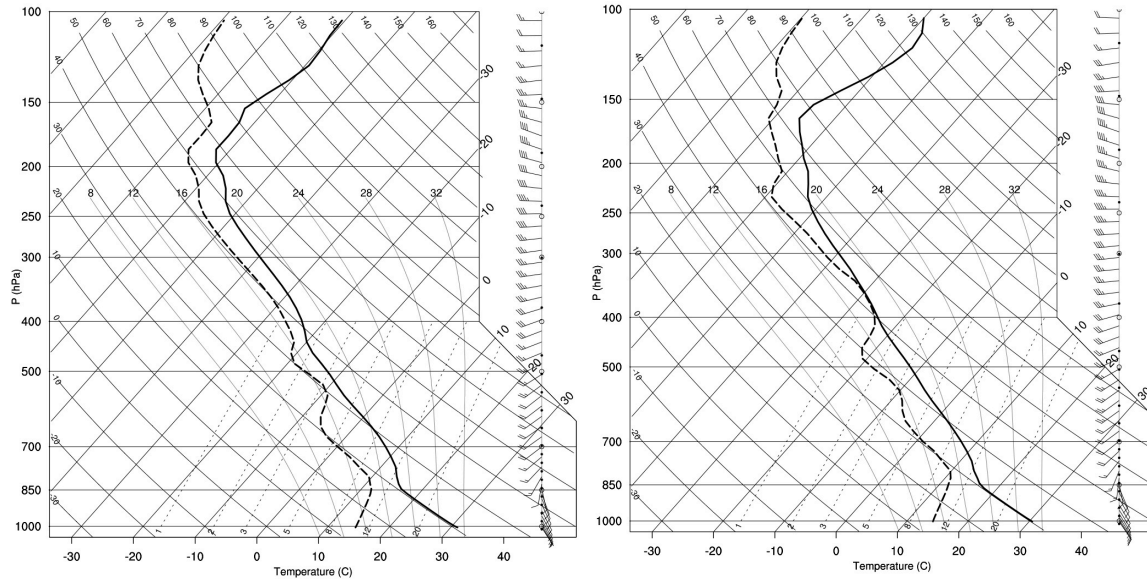


Fig. 9. Model derived soundings of the inflow environment for 18 May 2010 for the single moment (left) and the two moment (right) microphysical parameterizations.

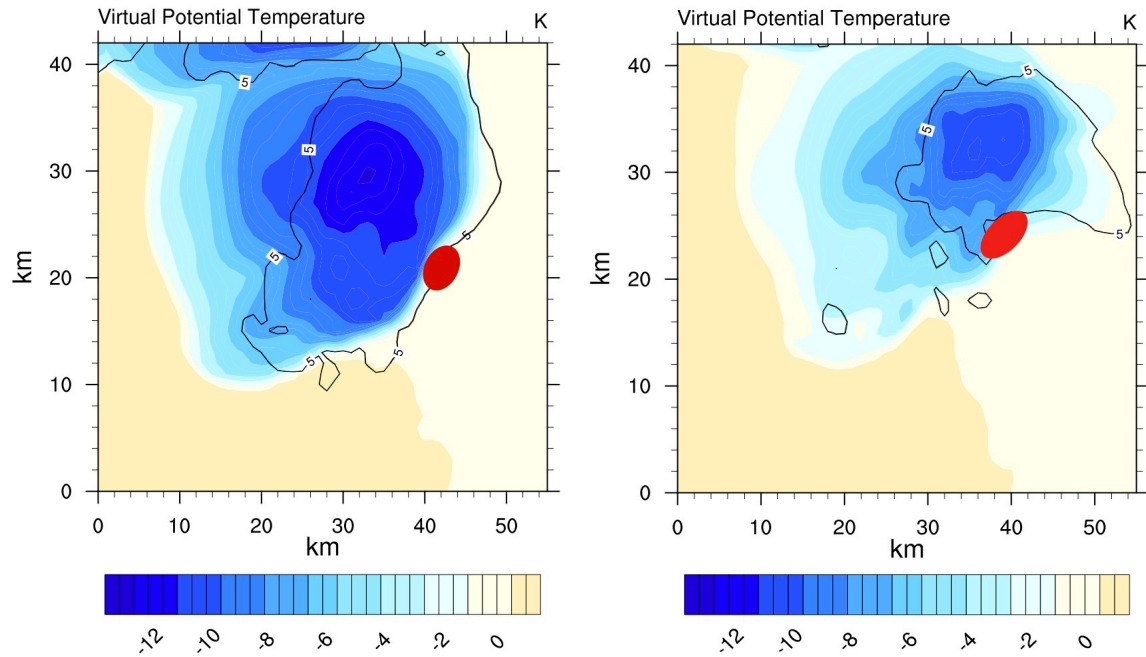


Fig. 10. Virtual potential temperature deficits (K) for the 18 May 2010 simulations at the lowest model level for simulations utilizing the single moment (left) and the two moment (right) microphysical parameterizations. The verification time is 2320 UTC. The red oval indicates the location of the mesocyclone.